

## AN34 Experiments in Nuclear Science Laboratory Manual Fourth Edition



### Experiment IV-7 High-Resolution Gamma-Ray Spectroscopy

# High-Resolution Gamma-Ray Spectroscopy

## Introduction

Gamma-ray energies will be measured with a High-Purity Germanium (HPGe) detector and research-grade electronics. The principles behind the response characteristics of the detector are explained. The high-resolution measurement results are contrasted with those obtainable from the NaI(Tl) (sodium iodide) scintillation detector previously explored in Experiment IV-3.

Most of the experiments in this series are written for use with lower-cost detectors and electronic modules. However, in this experiment, which illustrates the superior resolution capabilities of the high-performance HPGe detector systems, research-grade signal processing modules have been incorporated to fully utilize the detector's capabilities.

Many colleges, universities, and national research laboratories have Nuclear Spectroscopy Centers that employ high-resolution gamma-ray spectrometry to investigate decay schemes of radioisotopes. Given the plethora of isotopes, opportunities continue to arise in exploring the details of the decay schemes. Improved energy resolution allows additional lines to be found in spectra. Occasionally, a doublet is discovered, whereas earlier measurements with NaI(Tl) detectors indicated only a single energy line.

High-Purity Germanium (HPGe) detectors are also extensively used to detect and monitor radioactivity in the environment, and to detect contraband radioisotopes and fissionable material. It is the excellent energy resolution of the HPGe detector that enables ultra-low detection limits in these applications.

Decay schemes for isotopes are included in refs. 10 and 12. More recent information on certain nuclei can be found in ORTEC's Nuclide Navigator Master Library software package (Model C53). An up-to-date on-line resource for such information is sponsored by:

National Nuclear Data Center  
 Building 197D  
 Brookhaven National Laboratory  
 Upton, NY 11973-5000  
 Phone: (631) 344-2902  
 Fax: (631) 344-2806  
 Email: nndc@bnl.gov  
 Internet: <http://www.nndc.bnl.gov>

In Experiment IV-3, gamma-ray spectroscopy with NaI(Tl) detectors was studied. The typical energy resolution that can be obtained with NaI(Tl) is circa 7% for the 0.662 MeV <sup>137</sup>Cs gamma-ray line. For NaI(Tl) detectors, the resolution is a strong function of energy. The resolution is primarily controlled by the statistical fluctuation of the number of photoelectrons produced at the photocathode surface in the photomultiplier tube. Table IV-7.1 illustrates some typical resolutions for a NaI(Tl) detector as a function of the gamma-ray energy. Note that it is conventional to express the resolution in percent for NaI(Tl) detectors.

Where

$$\% \text{ Resolution (FWHM)} = \frac{\delta E}{E} \times 100\% \approx \frac{k \times 100\%}{\sqrt{E}} \quad (1)$$

E is the energy of the peak,

δE is the FWHM of the peak in energy units, and

k is a proportionality constant characteristic of the particular detector.

The development of germanium detectors in the late 1960s completely revolutionized gamma spectroscopy. Fig. IV-7.1 illustrates the striking contrast in results obtained with the two common types of gamma-ray detectors. Compared to NaI(Tl), there is a factor of 30 improvement in the full-width at half-maximum (FWHM) resolution. As a result of this improved resolution, many nuclear energy levels that could not be resolved with NaI(Tl) detectors are easily identified by using HPGe detectors.

**Table IV-7.1. Typical Resolutions of a NaI(Tl) Detector for Various Gamma-Ray Energies.**

Isotope	Gamma Energy (keV)	Resolution (%)
<sup>166</sup> Ho	81	16.19
<sup>177</sup> Lu	113	13.5
<sup>133</sup> Te	159	11.5
<sup>177</sup> Lu	208	10.9
<sup>203</sup> Hg	279	10.14
<sup>51</sup> Cr	320	9.89
<sup>198</sup> Au	411	9.21
<sup>7</sup> Be	478	8.62
<sup>137</sup> Cs	662	7.7
<sup>54</sup> Mn	835	7.26
<sup>207</sup> Pb	1067	6.56
<sup>65</sup> Zn	1114	6.29
<sup>22</sup> Na	1277	6.07
<sup>88</sup> Y	1850	5.45

The information for this table was taken from *IRE Trans. Nucl. Sci.* **NS-3**(4), 57 (Nov. 1956). "Intrinsic Scintillator Resolution," by G. G. Kelley *et al.*, quoting results from F. K. McGowan, *et al.*

# High-Resolution Gamma-Ray Spectroscopy

Concurrently, the development of lithium-drifted silicon detectors [Si(Li)] with drastically-improved energy resolution revolutionized x-ray spectrometry. These Si(Li) devices are studied in Experiment IV-8.

The purpose of this experiment is to explore some of the properties of HPGe detector systems. This experiment deals only with the practical aspects of making measurements with these detectors. To understand the properties of these detector systems, the following brief review of gamma-ray interactions and pair-production processes is included.

## Gamma-Ray Interactions in HPGe Detectors

Fig. IV-7.2 shows graphs for the three important gamma-ray interactions in both germanium and silicon. The absorption cross sections for germanium are of interest in this experiment. The corresponding values for silicon will be used in Experiment IV-8.

When a gamma-ray photon enters a detector, it must produce a recoil electron by one of three processes before it is recorded as an event: (1) the photoelectric effect, (2) the Compton effect, or (3) pair production.

In the **photoelectric process**, the gamma-ray or x-ray photon transfers all of its energy to an electron in the detector. Consequently, the photon vanishes. The recoiling electron loses energy by causing ionization of the detector material, resulting in a trail of electron-hole pairs. The bias voltage applied across the detector sweeps the electrons and holes to opposite electrodes, where the charge is collected to form the preamplifier pulse. For the photoelectric process, the total charge in the output pulse from the detector is proportional to the energy of the gamma-ray or x-ray that produced the interaction. These events will show up as full-energy photopeaks in the spectrum.

In the **Compton process**, the photon is scattered from an electron that is essentially not bound to an atom. Because the scattering angle can vary from 0 to 180 degrees, there is a range of energies that can be transferred from the photon to the recoiling electron. The scattered photon survives and carries off the remainder of the energy. It is the recoiling electron that loses energy by ionizing the detector material. Consequently, the charge collected from the detector will yield a distribution of pulse amplitudes at the preamplifier output up to some maximum pulse height. This maximum pulse height corresponds to the Compton edge in the energy spectrum, as explained in Experiment IV-3. There is a statistical probability that each Compton scattering event has an approximately equal chance to produce a pulse with any height up to this maximum. Thus, Compton events will provide a well-distributed low-energy continuum in the spectrum.

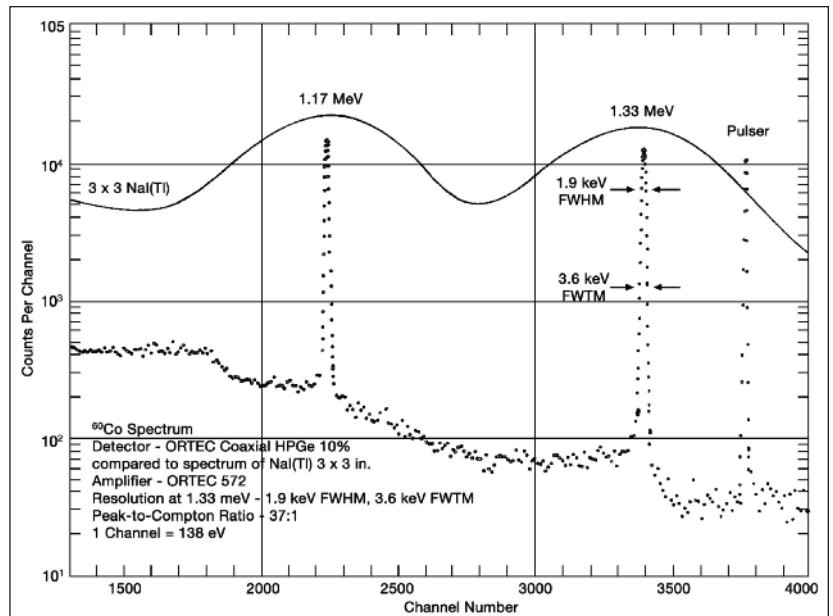


Fig. IV-7.1. A Portion of a  $^{60}\text{Co}$  Spectrum, Illustrating the Energy Resolutions and Peak-to-Compton Ratios for a Coaxial HPGe Detector Compared to a NaI(Tl) Detector.

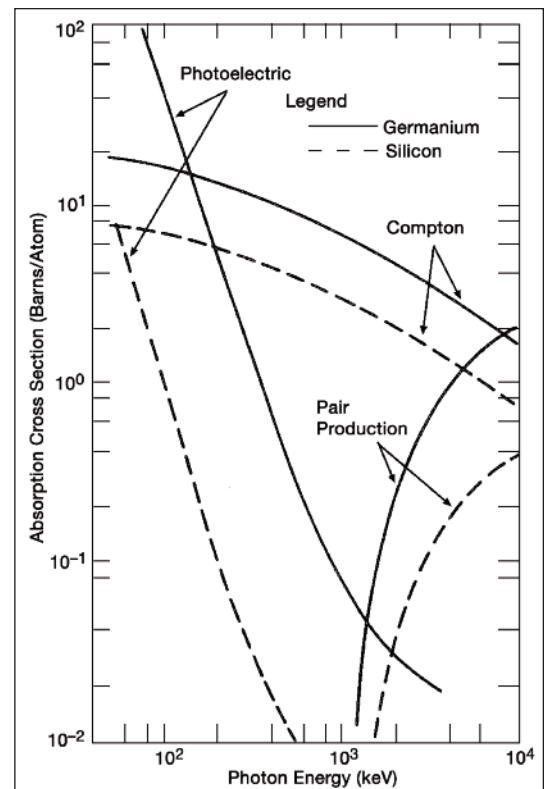


Fig. IV-7.2. Relative Probability (Cross Sections in Barns/Atom) for Each of the Three Types of Gamma-Ray Interactions in Ge and Si as a Function of Energy.

# High-Resolution Gamma-Ray Spectroscopy

In large detectors with high peak-to-Compton ratios, some Compton events also contribute to the full-energy peak, when the scattered photons undergo one or more additional interactions, and finally terminate in complete absorption by the photoelectric interaction.

The **pair-production process** can also provide a total absorption of the gamma-ray energy. The gamma-ray photon enters the detector and creates an electron-positron pair. All the energy of the initial photon is transferred to the electron-positron pair. Consequently, the initial photon disappears in the process. From the law of conservation of mass and energy, it follows that the initial gamma-ray must have an energy of at least 1.022 MeV, because it takes that much energy to create both the negative and positive electrons. The net mass that is produced is two electron masses, and this satisfies the law of conversion of energy,  $E$ , into mass,  $m$ , i.e.,  $E = mc^2$ . If the initial photon has an energy in excess of 1.022 MeV, that excess energy is transferred into the recoil energies of the positron and electron. Both the positron and the electron lose energy by causing ionization of the atoms in the detector. Once the positron is moving slowly enough, it can be captured by a free electron, and the two can combine. In this annihilation of the positron with an electron, both particles disappear, and their rest mass energies are converted into two photons travelling in opposite directions, with each photon having an energy of 511 keV. Note that the sum of the energies of these two annihilation gamma rays is 1.022 MeV.

The optional experiment IV-7.4 explores this process of positron annihilation when the positron is obtained from  $\beta^+$  decay of a  $^{22}\text{Na}$  radioactive source.

Fig. IV-7.3 illustrates what happens in the detector in the pair-production process. In Fig. IV-7.3 the  $e^-$  [ordinary electron] will produce a pulse whose magnitude is proportional to the energy of  $e^-$ , i.e.,  $E_{e^-}$ . The positron,  $e^+$ , will produce a pulse proportional to its energy,  $E_{e^+}$ . Since these two pulses are produced simultaneously, the output pulse from the detector would be the sum of the two pulses. When the positron annihilates in the detector, the annihilation radiation  $\gamma_1$  and  $\gamma_2$ , will be produced. In Fig. IV-7.3, both  $\gamma_1$  and  $\gamma_2$  are shown escaping from the boundaries of the detector without making any further interactions. [Note:  $E_{\gamma_1} = E_{\gamma_2} = 0.511$  MeV]. Thus, in this example, an energy of exactly 1.022 MeV escapes from the detector, and is subtracted from the total energy that entered the detector. It is

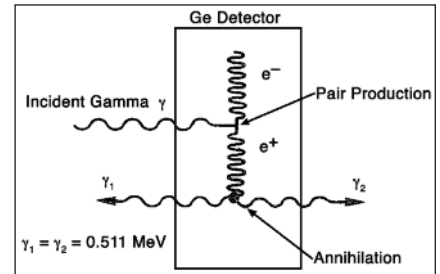


Fig. IV-7.3. The Process of Pair Production in a Ge Detector.

possible for only one, either  $\gamma_1$  or  $\gamma_2$ , to make a photoelectric interaction in the detector while the other escapes. In such cases, the total energy absorbed is 0.511 MeV less than the original incident gamma-ray energy. It is also possible for both gammas to make photoelectric interactions without escaping, with all the original energy being left in the detector. Therefore, in the spectrum being measured, there will be three peaks for each incident gamma-ray having an energy well in excess of 1.022 MeV. These peaks, labeled Full-Energy Peak, Single-Escape Peak, and Double-Escape Peak, will be separated by 0.511 MeV increments. Fig. IV-7.4 shows a typical spectrum that would be obtained for an incident gamma-ray energy of 2.511 MeV. The lower end of the spectrum that shows the Compton distribution has not been included. The Single-Escape Peak occurs at 2.00 MeV [ $E_\gamma - 0.511$  MeV], and the Double-Escape Peak occurs at 1.49 MeV [ $E_\gamma - 1.022$  MeV]. Of course, the full-energy peak represents those events for which there was a combination of pair production and photoelectric effect in which all the energy was absorbed in the detector.

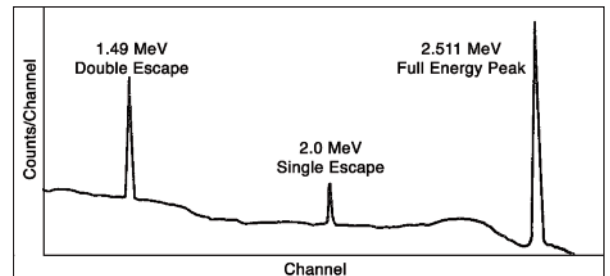


Fig. IV-7.4. Typical Spectrum for an Incident Gamma-Ray Energy of 2.511 MeV, Showing the Full-Energy, Single-Escape, and Double-Escape Peaks.

Now refer again to Fig. IV-7.2, and specifically to the curves for the interaction in germanium. The absorption cross section, plotted in the  $y$  direction, is a measure of the relative probability that an interaction will occur in a thin slab of the germanium detector. These probabilities of relative interactions, for the most part, determine the shape of the observed spectrum. For example, a photon with an energy of 100 keV has an absorption cross section of approximately 55 barns/atom for the photoelectric process. The corresponding Compton cross section is about 18 barns/atom. There is no pair production. These two cross sections are in the approximate ratio of 3:1, at 100 keV, implying that there are 3 times as many photoelectric interactions as Compton interactions. Fig. IV-7.5 shows the shape of a spectrum that could be expected for measurement of the 100 keV energy events.

# High-Resolution Gamma-Ray Spectroscopy

The shape of the spectrum changes drastically from 100 keV to 1 MeV. Fig. IV-7.6 shows the gamma spectrum that could be expected for the 1 MeV gammas incident on a thin HPGe detector. From Fig. IV-7.2, the ratio of Compton cross section to photoelectric cross section is approximately 90; so, in Fig. IV-7.6, the sum of the counts in the Compton distribution is  $\Sigma_c = 90,000$  and the sum of the counts in the photopeak is  $\Sigma_{pp} = 1000$ .

The relative efficiencies for HPGe and Si(Li) detectors can also be approximated from Fig. IV-7.2. For example, at  $E_\gamma = 400$  keV the photoelectric cross section for germanium is 6 barns/atom, and that for silicon is approximately 0.1 barn/atom. This is a ratio of 60:1, and indicates that there will be 60 times as many counts under the photopeak for a germanium detector as for a silicon detector at 400 keV, assuming that the detectors are the same size. This ratio of detector efficiencies reflects the fact that the photoelectric cross section varies as  $Z^5$ , where  $Z$  is the atomic number of the absorbing material. The atomic number of Ge is 32 and for Si it is 14. The ratio of these two numbers raised to the 5th power is 62.2, which agrees remarkably well with the above cross-section ratios. Higher atomic numbers offer greater photopeak efficiencies.

Fig. IV-7.2 shows that the cross-section for photoelectric absorption drops rapidly with increasing energy. From 300 keV to 3 MeV, the Compton-scattering cross-section dominates. The higher the energy, the more deeply the gamma-ray can penetrate the detector before it interacts with an electron. Consequently, the efficiency can be improved by increasing the dimensions of the Ge detector along the original direction of the photon, and in directions perpendicular to the path of the photon. According to the Beer-Lambert law for absorption [Experiments IV-2 and IV-3], a larger detector increases the probability that the photon will interact in the detector. If the initial interaction is a Compton scattering, the larger detector dimensions improve the chances that the scattered photon will be stopped by a photoelectric absorption before it leaves the detector volume, placing the event in the full-energy peak. Consequently, a larger detector improves the ratio of counts in the full-energy peak to the counts in the Compton continuum. This improves detection limits for weak peaks that would be obscured by statistical fluctuations in the Compton continuum from higher-energy gamma rays.

## Detector Structure

Basically, a HPGe detector is a very large semiconductor diode, with a reverse bias voltage applied to its two electrodes to deplete virtually all free charge carriers from the bulk of the detector. Small detectors can be obtained in the planar geometry that is similar to the structure of the silicon charged-particle detectors studied in experiments IV-4, IV-5 and IV-6. Figure IV-7.7 illustrates the planar geometry. The detector is a cylinder of HPGe with electrodes applied to its two circular ends.

Significantly larger detectors benefit from using the coaxial geometry depicted in Fig. IV-7.8. The P-type HPGe (GEM) is the type of detector used in this experiment. The detector is composed of a large cylinder of high-purity germanium. A hole is drilled from one end, along the centerline of the cylinder. One electrode is applied to the outer surface of the cylinder and to the closed end. The other electrode is applied to the inside surface of the central hole. The surface of the end from which the hole is drilled (open end) is passivated to reduce surface leakage currents between the two electrodes. The coaxial detector shape is mounted in the end cap of the cryostat, with the cylindrical axis of the detector diode aligned coaxially with the centerline of the end cap. The closed end of the detector is located a few millimeters behind the circular surface of the end cap.

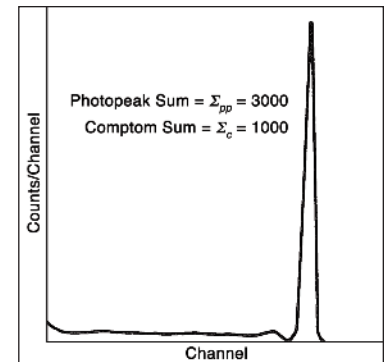


Fig. IV-7.5. A Typical Spectrum Expected for a 100 keV Photon in a Thin HPGe Detector.

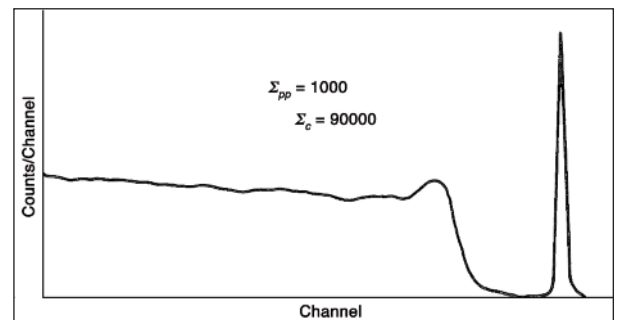


Fig. IV-7.6. A Typical Spectrum Expected for a 1 MeV Photon in a Thin HPGe Detector.

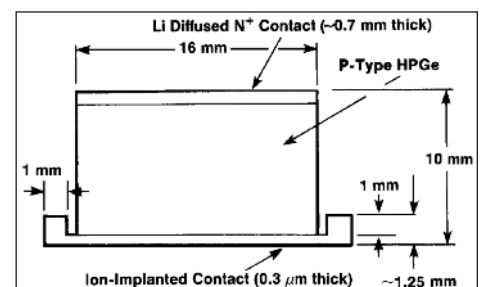


Fig. IV-7.7. The Structure of a 16 mm Diameter, 10 mm Deep Planar Detector.

# High-Resolution Gamma-Ray Spectroscopy

The detector and the first amplifying stage of the preamplifier are operated near the boiling temperature of liquid nitrogen (77°K) to reduce noise. Consequently, the detector and the first stage of the preamplifier are mounted in a vacuum cryostat. The cryostat establishes operation at the desired low temperature via a copper cooling rod dipped in the liquid nitrogen contained in the associated dewar. Operation at the cryogenic temperature dramatically reduces the leakage current in the HPGe detector and also diminishes thermally generated noise in the FET input stage of the preamplifier. The preamplifier feedback capacitor and feedback resistor are also cooled to reduce their noise contribution. As will be seen next, decreasing these sources of noise improves the energy resolution.

## Energy Resolution

The energy resolution of a HPGe detector is described by equation (2).

$$\Delta E_{\text{total}} = \sqrt{(\Delta E_{\text{noise}})^2 + (\Delta E_{\text{ion}})^2 + (\Delta E_{\text{incomplete}})^2} \quad (2a)$$

where

$$\Delta E_{\text{ion}} = 2.35\sqrt{\epsilon FE} \quad (2b)$$

$\Delta E_{\text{total}}$  is the full width at half maximum amplitude (FWHM) of the gamma-ray peak at energy E in the spectrum.  $\Delta E_{\text{noise}}$  is the contribution from the noise caused by the detector leakage current and the preamplifier. It is most readily measured as the FWHM of a pulser peak artificially introduced into the spectrum by injecting a pulser signal into the input of the preamplifier. The noise contribution is independent of the gamma-ray energy. But, it does depend on the shaping time constant of the spectroscopy amplifier. If the shaping time constant is too small or too large, the noise contribution will be higher than the optimum. Check the detector data sheet for the optimum shaping time constant to minimize the noise. The optimum will likely lie in the range of 3 to 6 microseconds.

$\Delta E_{\text{ion}}$  describes the variation in the number of electron-hole pairs generated as a result of ionization statistics. It depends on the average energy required to create an electron-hole pair (i.e.,  $\epsilon = 2.95$  eV), the energy of the gamma-ray, E, and the Fano factor, F. Note that the same units of energy must be used throughout equation (2). The Fano factor accounts for the fact that the ionization process lies somewhere between completely independent random ionization events at one extreme ( $F = 1$ ), and an absolutely deterministic conversion of energy into electron-hole pairs at the other extreme ( $F = 0$ ). For HPGe a Fano factor,  $F \approx 0.1$ , indicates the process is closer to the latter than the former condition.

$\Delta E_{\text{incomplete}}$  accounts for the variation in the ability to collect all of the electron-hole pairs that are created by the ionization process. Primarily, this applies to electron-hole pairs that recombine before they can be collected, or charge carriers that fall into traps while drifting to their respective electrode. Additionally, there is potential for a ballistic deficit effect when the shaping time constant is too small. For large coaxial HPGe detectors the charge collection time can vary from 50 to 700 ns, depending on the position at which the charge was created. If the amplifier shaping time constant is not large compared to these collection times, the pulse height will show additional fluctuations caused by random variations in the charge collection times. If the incomplete charge collection term is ignored in equation (2), spectral resolution measurements may lead to an inflated value for the implied Fano factor.

## Maximum Counting Rate Deduced from the Percent Dead Time

Because gamma rays arrive at the detector with random spacing in time, the width of the pulse from the amplifier limits the counting rate that can be processed without distortion. Probably the most efficient way to ensure that the maximum counting rate is not exceeded is to adjust the source-to-detector distance so that the percent dead time observed on the Multichannel Analyzer is less than 63%. The dominant dead time in the gamma-ray spectrometer specified for this experiment is a paralyzable (a.k.a., extending) dead time (ref. 11, 14 and 15). For a paralyzable dead time, the maximum analyzed throughput is accomplished when the dead time is 63%. Operation at counting rates that yield slightly less than 63% dead time will provide optimum performance.

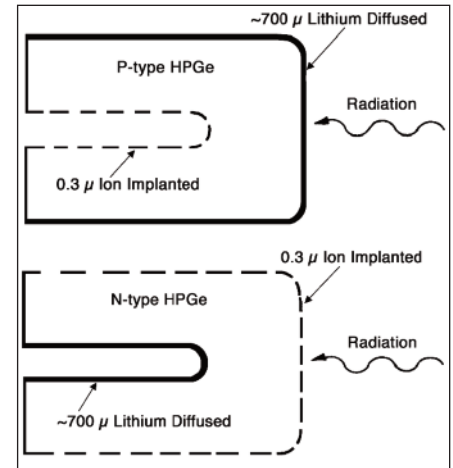


Fig. IV-7.8. Configurations of Coaxial Germanium Detectors.

# High-Resolution Gamma-Ray Spectroscopy

## Further Information on HPGe Detectors

Consult references 11, 13, 14 and 15 for further details on HPGe detectors.

## Equipment Required

<ul style="list-style-type: none"> <li>• <b>GEM10P4-70/CFG-PV4/DWR-30</b> Coaxial High Purity Germanium (HPGe) Detector (includes detector, preamplifier, cryostat, liquid-nitrogen dewar, and 12-ft. cable pack); typical specifications: 10% relative efficiency, 1.75 keV resolution at 1.33 MeV, 41:1 peak-to-Compton ratio. (Other ORTEC HPGe detector models may be substituted.)</li> <li>• <b>DSPEC-LF-POSGE</b> DSPEC-LF Digital Signal Processing Based Gamma-Ray Spectrometer with MAESTRO and DIM-POSGE HV module. (Other models of ORTEC spectrometer may be substituted but may result in minor differences to this script.)</li> <li>• <b>GF-057-M-20*</b> 20 <math>\mu\text{Ci}</math> <math>^{57}\text{Co}</math> (272-d half life). A license is required for this source.</li> <li>• <b>GF-137-M-20*</b> 20 <math>\mu\text{Ci}</math> <math>^{137}\text{Cs}</math> (30-y half life). A license is required for this source.</li> </ul>	<ul style="list-style-type: none"> <li>• <b>GF-060-M-10*</b> 10 <math>\mu\text{Ci}</math> <math>^{60}\text{Co}</math> (5.3-y half life). A license is required for this source.</li> <li>• <b>GF-228-D-10*</b> 10 <math>\mu\text{Ci}</math> <math>^{228}\text{Th}</math> (698-d half life). A license is required for this source.</li> <li>• Personal Computer with USB port and Windows operating system.</li> </ul> <p><b>OPTIONAL FOR EXPERIMENT IV-7.4</b></p> <ul style="list-style-type: none"> <li>• <b>POSK22-10*</b> 10 <math>\mu\text{Ci}</math> <math>^{22}\text{Na}</math> thin source for observing positron annihilation peak broadening. A license is required for this source.</li> <li>• <b>Foil-AL-30</b> 10 ea 1/2-inch (1.27-cm) dia. Aluminum foils, 0.030-inch (0.076 cm) thick</li> <li>• <b>Foil-NI-10</b> 10 ea 1/2-inch (1.27-cm) dia. Nickel foils, 0.010-inch (0.025 cm) thick</li> </ul>
---	--

\*Sources are available direct from supplier. See the ORTEC website at [www.ortec-online.com/Service-Support/Library/Experiments-Radioactive-Source-Suppliers.aspx](http://www.ortec-online.com/Service-Support/Library/Experiments-Radioactive-Source-Suppliers.aspx)

## EXPERIMENT IV-7.1. Energy Resolution with a HPGe Detector

**CAUTION:** The instructor will provide the HPGe detector and instructions for its use. Before attempting to use the detector, carefully read the instruction manual. This is a very expensive detector system and must be handled very carefully.

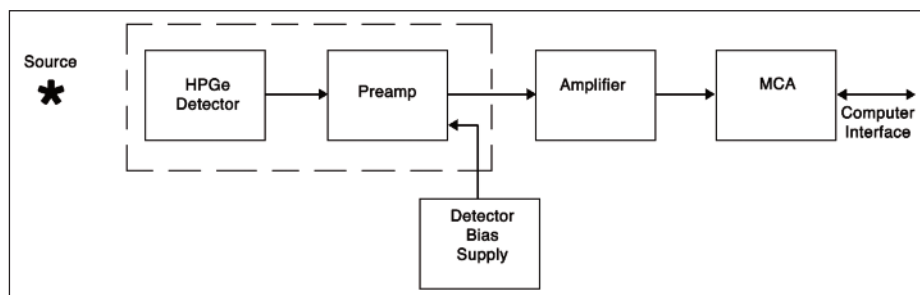


Fig. IV-7.9. Function System Block Diagram for the Gamma-ray Spectrometer.

## Procedure

1. Your instructor should have already cabled up the system. The required steps are:

Referring to the equipment list above, the MAESTRO software should be installed on the PC according to the installation instructions and there should be an ICON on the desktop (Fig. IV-7.10).

The DSPEC-LF spectrometer should be cabled to the USB port of your computer, and the DIM-POSGE HV module should be connected to the DSPEC-LF via the thick cable and to the detector coaxial cable set.

2. The MAESTRO setup procedure should have been run to establish communication between your computer and the DSPEC-LF. Click the MAESTRO ICON and verify that communication is being established.



Fig. IV-7.10. MAESTRO

# High-Resolution Gamma-Ray Spectroscopy

If the display looks like Fig. IV-7.11, with the “Mcb Model No” present at position 1, and if position 2 looks similar to that shown in Fig. IV-7.11, then communication is established. If position 2 looks like Fig. IV-7.12 then there is no communication and you should consult your instructor or the system documentation.

3. On the MAESTRO display, select Acquire/MCB Properties and select the High Voltage tab (Fig. IV-7.13).

The target voltage should be as specified on the Detector Quality control (QAD) sheet. Assuming that to be the case, enable the HV by clicking the “ON” button. Now check the other Properties tabs. In general the default settings should be correct.

4. Select the Amplifier tab (Fig. IV-7.14). These parameters should suffice for the equipment specified. The optimize function adjusts the pole zero and flat top settings to their optimum values. These optima vary from detector to detector, and in the past Pole Zero adjustment was a tricky procedure requiring the use of an oscilloscope. Place the  $^{60}\text{Co}$  source close enough to the detector to create a count rate of  $\sim 1000\text{cps}$  as registered on the MAESTRO input count rate meter, available in the Calculate menu. Click on Start Auto for the optimize function and the Pole Zero and Flat top will optimize themselves after a few seconds.
5. Select the Amplifier 2 tab (Fig. IV-7.15). A rise time of  $12\ \mu\text{s}$  and a Flat top width of 0.8 is suitable for a small HPGe detector. More information on these functions is provided in the ORTEC system user manuals. The optimized Pole Zero and Tilt values will be displayed following step 4. “Insight” starts a digital oscilloscope mode to allow display of the digital synthesized wave forms after the application of the digital filter. If time allows, you might want to return and experiment with that later, (you will need the ORTEC Manual).

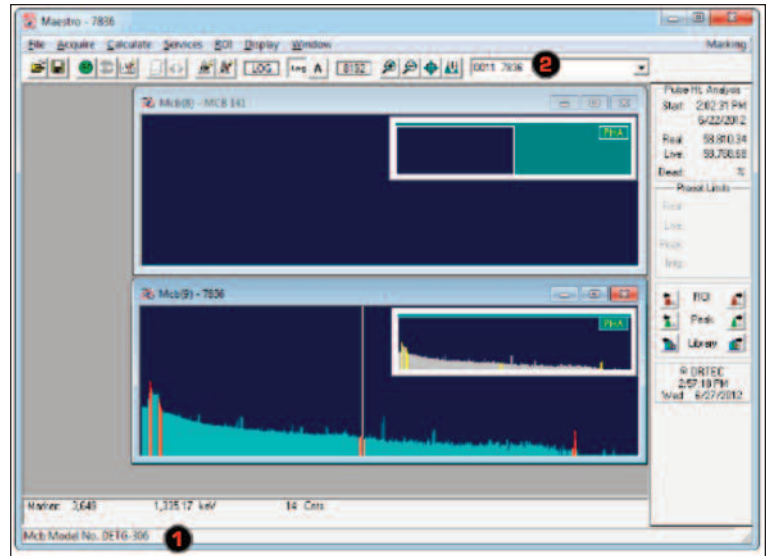


Fig. IV-7.11. MAESTRO Display.

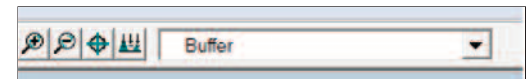


Fig. IV-7.12. Communication Not Established.

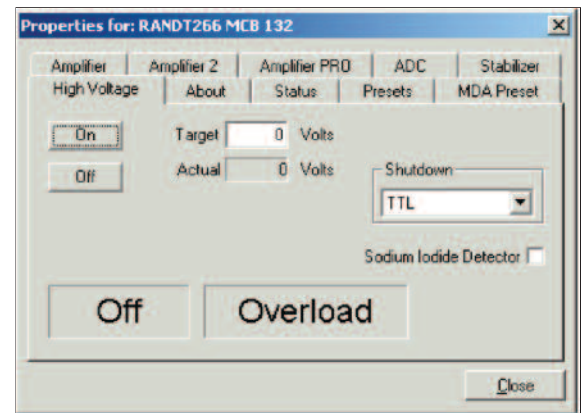


Fig. IV-7.13. High Voltage Display.

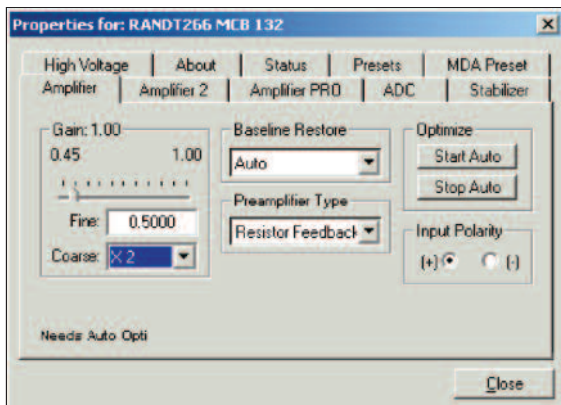


Fig. IV-7.14. Amplifier Display.

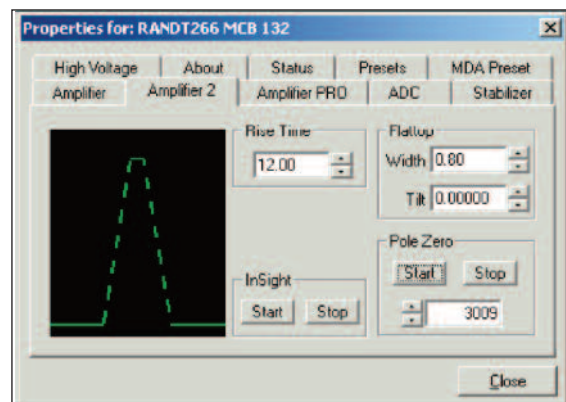


Fig. IV-7.15. Amplifier 2 Display.

# High-Resolution Gamma-Ray Spectroscopy

- Select the ADC tab (Fig. IV-7.16). Check that the settings are as in the figure, but adjust the Conversion Gain setting to 8192. The Upper Level Discriminator should be set just below this value.
- Adjust the Gain for Recording Spectra. Start the Acquisition of data using MAESTRO (Hint: "ALT 1" is a convenient shortcut), and observe the spectrum on the live display.

Figure IV-7.17 shows the characteristic  $^{60}\text{Co}$  spectrum with the two lines at 1173 keV and 1332 keV. The third high energy line is due to natural  $^{40}\text{K}$  at 1460 keV which may or may not be present in your spectrum.

Adjust the amplifier gain until the spectrum looks like Fig. IV-7.17. Place the upper  $^{60}\text{Co}$  peak around about channel 5300. Accelerator keys allow this adjustment to be made while observing the spectrum:

- ALT+ increases the gain one increment
- ALT- decreases the gain one increment
- SHIFT ALT + increases the gain several increments
- SHIFT ALT - decreases the gain several increments
- ALT 1 starts an acquisition
- ALT 2 Stops an acquisition
- ALT 3 clears acquired or acquiring data

- Make an acquisition on the MCA for a long enough period of time to create a well-defined spectrum as illustrated in Fig. IV-7.17.

- Calibrate the energy scale of the MCA using the MAESTRO "calibrate function" as follows:

- Position the cursor below the 1173 keV peak. Press "CTRL >" to jump the cursor to the top of the peak and press the "Ins" key on your computer keyboard. This will mark a region of interest around the peak.
- Jump to and mark the 1332 keV peak by repeating the process.
- Select Calculate/Calibration/Destroy Calibration to remove any calibration which may be present. Then enter the energy of the currently selected peak 1332.5 keV of the upper  $^{60}\text{Co}$  peak.
- Index down to the lower peak ("SHIFT <") and repeat entering 1173.238 keV as the energy. Now select "keV" as the units for the calibration.

- The system is now calibrated based on these two points. Note that the cursor now presents both marker channel and corresponding energy, as well as the count content of the channel at the bottom of the screen.

- Select Calculate/Peak info to display peak parameters similar to Figure IV-7.18. FWHM is the peak width or "full width half maximum" expressed in keV.

- Save the spectrum for future reference.

- Add the  $^{57}\text{Co}$ , and  $^{137}\text{Cs}$  sources to the  $^{60}\text{Co}$  source, and acquire a composite spectrum. Make sure the dead time is not excessive (< ~50%) and acquire a spectrum long enough to have several hundred counts in the major peaks.

- Using the MAESTRO functions from previous steps, determine the Energy and FWHM of the major peaks in the spectrum: 122 keV, 662 keV, 1173 keV, 1332 keV.

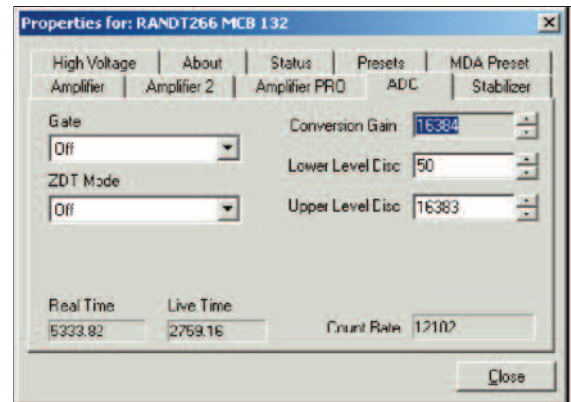


Fig. IV-7.16. ADC Display.

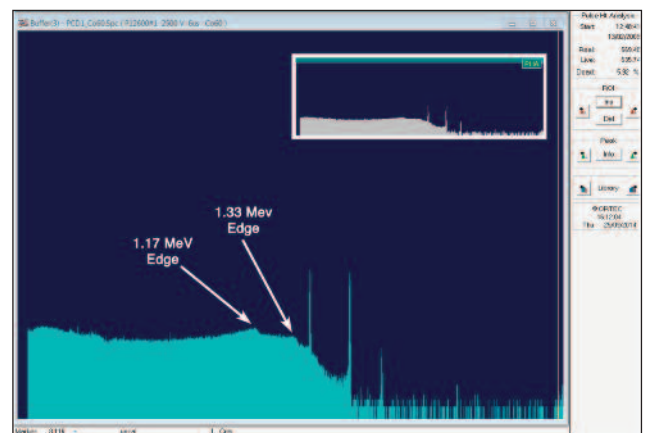


Fig. IV-7.17.  $^{60}\text{Co}$  Spectrum.

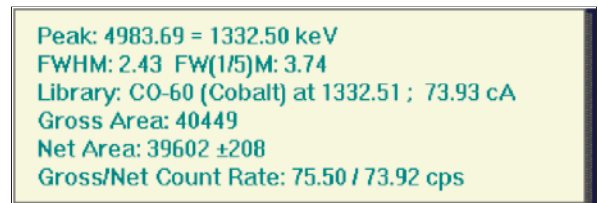


Fig. IV-7.18. Peak Info Display.

# High-Resolution Gamma-Ray Spectroscopy

## EXERCISES

- What is the FWHM resolution in keV for the two photopeaks? How does the 1332 keV value compare with the detector's resolution specifications?
- From the  $^{60}\text{Co}$  spectrum, determine the energies of the Compton edges associated with the two gamma-ray energies. How do these compare with the values that were calculated from the formula used in Experiment IV-3?
- Tabulate the data from Step 14. FWHM is  $\Delta E_{\text{total}}$  from Eq 2a. Use this as the column heading.  
Substituting equation 2b into 2a and squaring both sides and assuming that  $\Delta E_{\text{incomplete}} = 0$ , Equations 2a and 2b may be combined as

$$(\Delta E_{\text{total}})^2 = (\Delta E_{\text{noise}})^2 + 5.5 \epsilon FE$$

- Add a column to your table for  $(\Delta E_{\text{total}})^2$
- Plot a graph of  $(\Delta E_{\text{total}})^2$  (y-axis) versus E (X-axis) from your tabulated data.
- Using the value  $\epsilon = 2.95$  calculate the value of F from the slope of the straight line and  $\Delta E_{\text{noise}}$  from the intercept.
- Comment on the values obtained, given that we have assumed that  $\Delta E_{\text{incomplete}} = 0$ .

## EXPERIMENT IV-7.2. Photopeak Efficiency and Peak-to-Compton Ratio

Compared to NaI(Tl) detectors, the energy resolution with HPGe detectors is better by a factor of 30 or more. This dramatic increase in resolution is sometimes coupled with a compromise of the photopeak efficiency, because the larger-volume HPGe detectors that deliver higher photopeak efficiency are much more expensive to manufacture. Thus a smaller, lower-efficiency, HPGe detector is employed with this experiment to reduce the cost. Normally, the efficiency listed for a HPGe detector is expressed as a ratio to the efficiency expected for a 3-inch x 3-inch NaI(Tl) detector. The standard method for comparing the efficiencies of HPGe detectors with NaI(Tl) detectors is to compare their counting rates at the 1.333 MeV line of  $^{60}\text{Co}$ , using a standard distance of 25 cm from the source to the detector face, and placing the source on the detector axial centerline.

The resolution of HPGe detectors is so many times better than that of NaI(Tl) that the ability to see a photopeak above the Compton distribution is remarkably enhanced. Consider a simple example in which the efficiencies of the HPGe and NaI(Tl) detectors are assumed to be the same. Presume that in a particular experiment, we observe 10,000 counts under the photopeak for each detector. If the resolution of the HPGe detector is 10 times better than the NaI(Tl) detector resolution, the HPGe detector will have a peak height that is 10 times the peak height exhibited by the NaI(Tl) detector. This relationship results because the area under the photopeak (10,000 in this example) is approximately proportional to the width times the height of the peak. Since the width of the HPGe peak is  $1/10$  the width of the NaI(Tl) peak, its height must be 10 times as great.

This example can be easily extrapolated to real situations where the advantages of superior resolution are very important. For example, Fig. IV-7.19 shows the striking differences for comparative spectra obtained on a mixed sample of  $^{76}\text{As}$ ,  $^{122}\text{Sb}$ , and  $^{124}\text{Sb}$  with the two types of detectors. Each of the closely spaced energy lines is shown separately in the HPGe spectrum, while they are all included in a single broad photopeak in the NaI(Tl) spectrum. In this experiment, we will measure some of these photopeak efficiencies and also determine the peak-to-Compton ratio for a HPGe detector.

The peak-to-Compton ratio is a pragmatic parameter that provides a relative comparison between the abilities of two different detectors to detect low-intensity peaks on the continuum caused by Compton scattering. It includes the effect of energy resolution and the full-energy peak efficiency of the detector. The peak-to-Compton ratio is the height of the 1.333 MeV full-energy peak from a  $^{60}\text{Co}$  source, divided by the height of the Compton continuum from that same spectrum between 1.040 and 1.096 MeV. HPGe detectors with a larger volume have a higher probability that the detected gamma-ray will end up in the full-energy peak, instead of the Compton continuum. That improves the peak-to-Compton ratio. Unfortunately, higher-volume detectors tend to have slightly worse energy resolution, and that detracts from the peak-to-Compton ratio. Fortunately, the improved efficiency tends to dominate the degraded energy resolution, causing higher-volume detectors to have better detection limits for low-activity peaks.

# High-Resolution Gamma-Ray Spectroscopy

## Procedure

1. Continue with the same equipment setup that was used for Experiment IV-7.1.
2. Place the  $^{60}\text{Co}$  source 25 cm from the end cap of the HPGe detector, and on the axial centerline of the detector.
3. Accumulate the spectrum in the MCA for a time period long enough to determine heights  $h_1$  and  $h_2$  to a fair degree of accuracy. In Fig. IV-7.20,  $h_1$  is the height of the 1.3332 MeV photopeak from the  $^{60}\text{Co}$  radioisotope, and  $h_2$  is the height for the Compton distribution, located just below the Compton edge (between 1.040 and 1.096 MeV). Read the data from the MCA.
4. Save the spectrum to the internal hard disk for potential use later.

### EXERCISE

- a. Calculate the peak-to-Compton ratio, which is  $h_1$  divided by  $h_2$  in Fig. IV-7.20. Compare your value with the specification for this detector. Check with your laboratory instructor for the record of the ratio.
5. Clear the spectrum from the MCA.
  6. Place a  $10\text{-}\mu\text{Ci}$   $^{60}\text{Co}$  source at a distance of exactly 25 cm from the face of the detector.
  7. Accumulate a spectrum for this source with approximately 3000 counts under the 1.333 MeV photopeak.
  8. Set a Region of Interest across the entire 1.333 MeV photopeak and read the total number of counts in the peak,  $\Sigma_{pp}$ . Also write down the elapsed live time for the spectrum,  $t_L$ .
  9. Save the spectrum on the internal hard disk for potential later use.

### EXERCISES

- b. Divide the number of counts in the 1.333 MeV photopeak by the elapsed live time. Call this counting rate  $R_1$ .

$$R_1 = \frac{\Sigma_{pp}}{t_L} \quad (3)$$

- c. The rate,  $R_1$  from Eq. (3) is to be compared with the rate,  $R_2$ , that is expected for the same source when it is located 25 cm from the face of a 3-in. x 3-in. NaI(Tl) detector. The efficiency of this size NaI(Tl) detector for a source-to-detector distance of 25 cm is given as  $\epsilon_2 = 1.2 \times 10^{-3}$ , (from "Gamma Ray Spectrum Catalog" by R. L. Heath, Idaho Falls Report IDO-16880). Using this efficiency number, the counting rate ( $R_2$ ), that you would observe under the photopeak for a 3-in. x 3-in. NaI(Tl) detector at 25 cm source distance is given by

$$R_2 = \epsilon_2 A \quad (4)$$

where  $A$  is the gamma-ray activity of the source in counts per second.

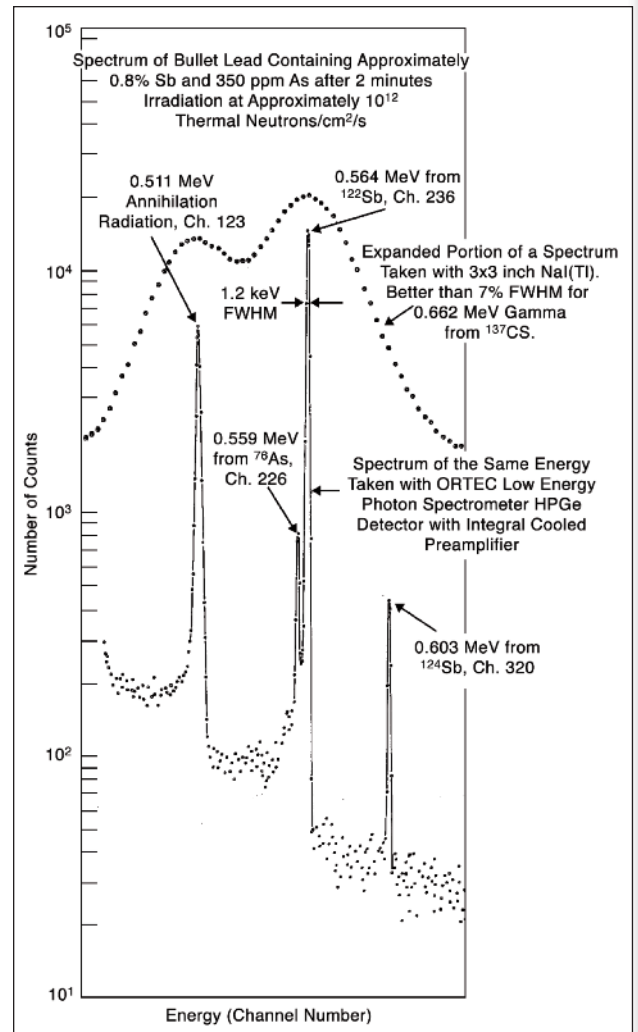


Fig. IV-7.19. Comparative Spectra Taken with HPGe and NaI(Tl) Detectors.

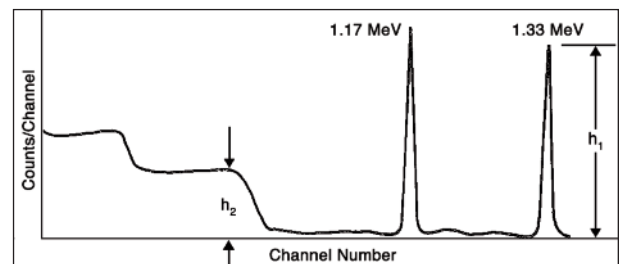


Fig. IV-7.20. Measuring the Peak-to-Compton Ratio on a  $^{60}\text{Co}$  Spectrum.

# High-Resolution Gamma-Ray Spectroscopy

Since  $^{60}\text{Co}$  has one 1.3332 MeV gamma ray for each decay, A is given by

$$A = 3.7 \times 10^4 \text{ a} \quad (5)$$

Where "a" is the source strength in microCuries ( $\mu\text{Ci}$ ).

$R_2$  can be calculated from equations (4) and (5). Subsequently, the relative photopeak efficiency for the HPGe detector is obtained from:

$$\text{Relative Photopeak Efficiency} = \frac{R_1}{R_2} \times 100\% \quad (6)$$

- d. Calculate the relative photopeak efficiency for your measurement, and compare it with the value that is specified for the detector. Check with your laboratory instructor for the record of the detector's efficiency.

## EXPERIMENT IV-7.3. Escape Peaks and Efficiency for HPGe Detectors

As discussed earlier, when an incident gamma-ray with sufficient energy enters the crystal it can create an electron-positron pair. When the positron annihilates, two gammas with equal energy at 0.511 MeV are produced which leave with an angular separation of  $180^\circ$ . In Fig. IV-7.3, these two gammas are shown as  $\gamma_1$  and  $\gamma_2$ . For small detectors, it is very probable that both  $\gamma_1$  and  $\gamma_2$  will escape from the detector before they make any further interactions in the crystal. The energy thus absorbed would be  $E_\gamma - 1.022 \text{ MeV}$ , and is shown as the Double-Escape Peak in Fig. IV-7.4. As the detector size increases, the probability is greater that either  $\gamma_1$  or  $\gamma_2$  will make a photoelectric interaction within the crystal. If one of these gammas does undergo a photoelectric interaction, the energy of the event that is recorded in the detector is the Single-Escape Peak in Fig. IV-7.4. For even larger detectors, the probability of both  $\gamma_1$  and  $\gamma_2$  being absorbed by photoelectric interactions is even greater, making it more likely that the total energy of the original gamma-ray is absorbed in the crystal.

Fig. IV-7.21 shows some measurements that have been made for coaxial and planar HPGe detectors. From this figure, the ratios of Full-Energy, Double-Escape Peak, and Single-Escape Peak efficiencies can be determined by inspection for the size of detector that is identified in the figure.

To see how the measurements were made for Fig. IV-7.21, consider the  $E_\gamma$  of 2.511 MeV shown in Fig. IV-7.4. Assume that the Compton distribution has been subtracted for each peak in Fig. IV-7.4, and that the following sums have been measured:

$\Sigma$  at Full Energy (2.511 MeV) = 6000,

$\Sigma$  at Single-Escape (2.00 MeV) = 1000

$\Sigma$  at Double-Escape (1.489 MeV) = 3000.

From these numbers the simple ratios can be obtained.

### Procedure

For this experiment, the same equipment setup that was used for Experiment IV-7.1 will be used. But, the energy calibration will be changed to accommodate the 2.614 MeV gamma-ray from the  $^{228}\text{Th}$  source. As detailed in Experiment IV-4,  $^{228}\text{Th}$  is part of a natural decay series that involves sequences of alpha and  $\beta^-$  decays, ultimately ending up with a stable  $^{208}\text{Pb}$  isotope. The 2.614 MeV gamma-ray is generated from an excited state in  $^{208}\text{Pb}$  near the end of that series, as  $^{208}\text{Tl}$  decays by alpha emission into  $^{208}\text{Pb}$ . Several gamma-ray sources,  $^{57}\text{Co}$ ,  $^{137}\text{Cs}$ , and  $^{60}\text{Co}$  will be used along with the  $^{228}\text{Th}$  source to establish the new energy calibration.

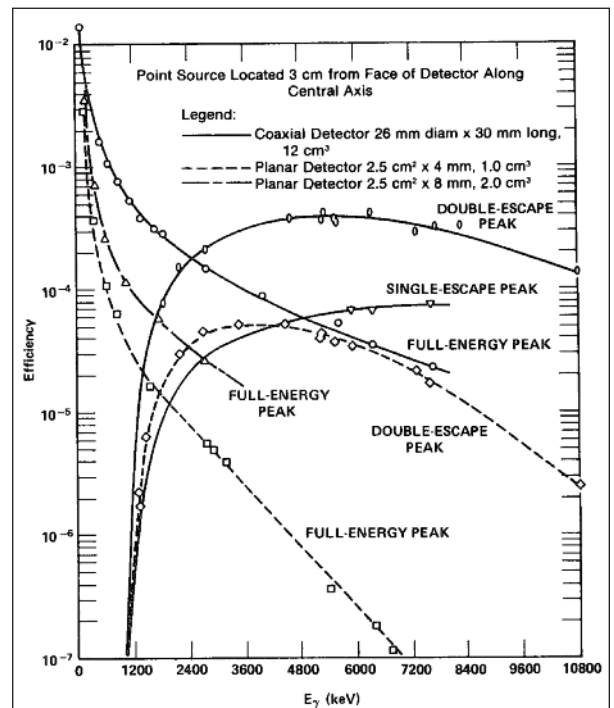


Fig. IV-7.21. Measured Full-Energy and Escape-Peak Efficiencies for HPGe Detectors of Different Sizes.

# High-Resolution Gamma-Ray Spectroscopy

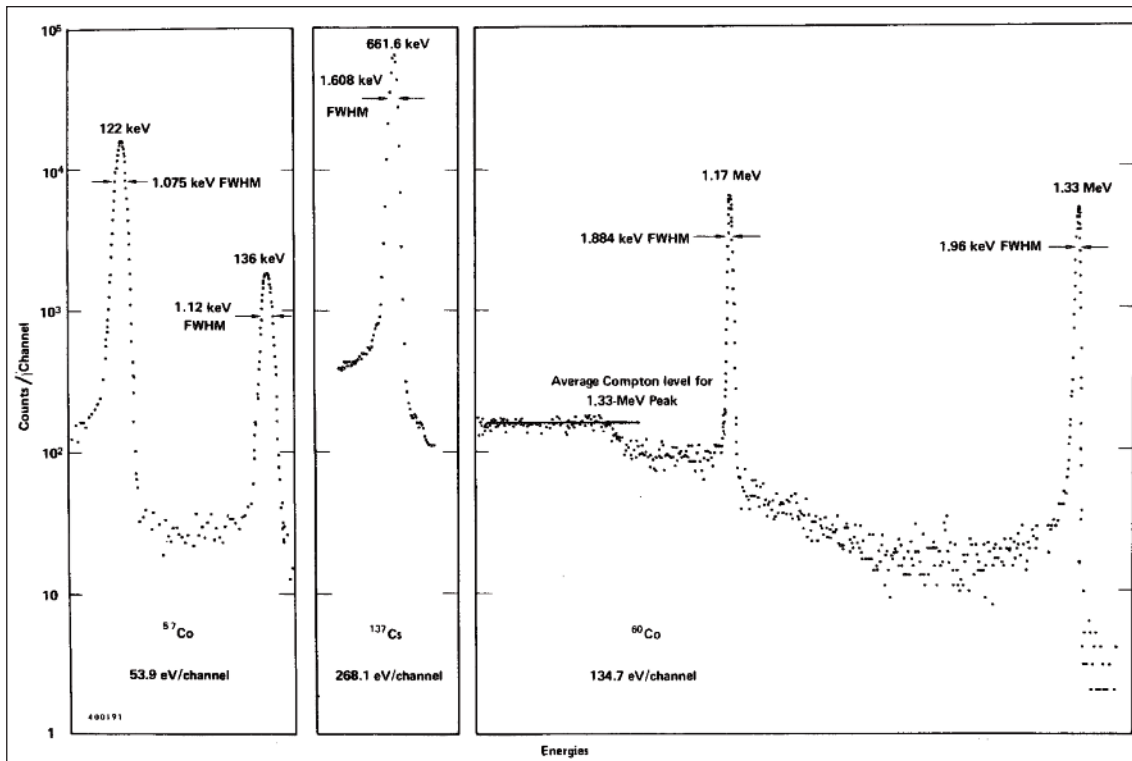


Fig. IV-7.22. Typical Spectra in the Full-Energy-Peak Regions for  $^{57}\text{Co}$ ,  $^{137}\text{Cs}$  and  $^{60}\text{Co}$  Acquired with a HPGe Detector.

1. Place the  $^{60}\text{Co}$  source in front of the detector. Adjust the amplifier gain so that the 1.333 MeV gamma-rays produce a 4.1 V pulse height on the oscilloscope.
2. Check that the percent dead time on the MCA is <63%. Adjust the source-to-detector distance to meet that condition, if necessary.
3. Acquire a spectrum with the  $^{60}\text{Co}$  source until the peaks are statistically well defined.
4. Measure the channel centroids of the 1.333 and 1.173 MeV peaks, and record them for energy calibration. The 1.333 MeV peak should be in the neighborhood of channel 3,342. If it deviates by more than 250 channels from this location, readjust the Amplifier gain to bring it into compliance. Save the spectrum for possible later reference.
5. Replace the  $^{60}\text{Co}$  source with the  $^{137}\text{Cs}$  source and acquire a spectrum. If necessary, adjust the source-to-detector distance to achieve <63% dead time. Measure the channel centroid of the 662 keV peak and record the value. Save the spectrum for possible future reference.
6. Replace the  $^{137}\text{Cs}$  source with the  $^{57}\text{Co}$  source. If necessary, adjust the source-to-detector distance to achieve <63% dead time. Acquire a spectrum. Measure the channel centroids of the 122 keV and 136.5 keV peaks, and record those values. Save the spectrum for possible future reference.
7. ALTERNATIVELY, the three sources can be combined into one spectrum for the energy calibration measurement. In this scheme, place the  $^{57}\text{Co}$  source directly on the center of the detector end-cap. Stack the  $^{137}\text{Cs}$  source on top of the  $^{57}\text{Co}$  source, and add the  $^{60}\text{Co}$  source on top of the  $^{137}\text{Cs}$  source. If necessary, adjust the source-to-detector distance to achieve <63% dead time. Acquire a spectrum for a sufficient length of time so that all the peaks of interest are statistically well defined above the background caused by the Compton continua. Save the spectrum for possible later reference.
8. Use the energy calibration feature of MAESTRO to calibrate the horizontal axis in keV or MeV. If employing the composite spectrum, make sure that you use the net area above the local background to compute the centroids.

# High-Resolution Gamma-Ray Spectroscopy

9. Remove the energy calibration sources and place the  $^{228}\text{Th}$  in front of the detector at a 3 cm distance from the detector along the axial centerline of the detector. If necessary, increase the source-to-detector distance to achieve <63% dead time. Accumulate a spectrum long enough to achieve statistically well-defined peaks for all of the major peaks of interest. Save the spectrum for future use.
10. If you plan to complete your report after you leave the laboratory, transfer all the saved spectra to a transportable storage device, such as a portable hard disk, memory stick, or CD for later analysis and plotting. The most efficient way to achieve this goal is to use the MAESTRO option to save [export] the spectrum as an ASCII file. The ASCII file can be imported into an Excel spreadsheet. Choose the Tab and Space Delineated option in Excel when importing the file. This generates the file header and the channel-by-channel counts as a table in Excel. That data can be plotted with the Excel graphing options, and labeling can be inserted on each peak in the spectrum. The resulting Excel graph can be imported into your lab report and printed. Another option for including spectra in your report is to capture an image of the spectra on the laboratory computer display using the FullShot image capture software provided with MAESTRO.

## EXERCISES

- a. Plot the  $^{228}\text{Th}$  spectrum with a logarithmic vertical [counts] scale and a linear horizontal [energy] scale. On the plot, identify all the major peaks and the corresponding escape peaks. Compare the energies you measured for these peaks with those that are listed for the source in references 10 or 12.
- b. Do the escape peaks associated with the 2.614 MeV gamma-ray occur at the correct energies? If not, does adding the 2.614 MeV gamma-ray and its escape peaks to the above energy calibration improve the agreement?
- c. Calculate the escape peak ratios. Define  $\Sigma_f$  as the sum of counts under the full-energy peak,  $\Sigma_1$  as the sum under the single-escape peak, and  $\Sigma_2$  as the sum under the double-escape peak. Be sure to subtract the background caused by the Compton distribution from these sums; then determine the ratios  $\Sigma_f/\Sigma_1$ ,  $\Sigma_f/\Sigma_2$ , and  $\Sigma_2/\Sigma_1$ . How do these ratios compare with those the laboratory instructor has for the  $^{228}\text{Th}$  source and the detector you are using?
- d. How will a different source-to-detector distance affect the escape peak ratios?

## EXPERIMENT IV-7.4. Doppler Broadening with Annihilation Radiation (Optional)

As previously discussed, when a positron combines with an electron, the pair annihilate each other and two 511 keV gamma rays are emitted in opposite directions. The rest masses of the positron and electron are converted to energy in the form of the two gamma rays. That is the simple picture. When examined in more detail, one finds that the process is sensitive to the binding energy of the electron in an atom, and the momenta carried by the positron and the electron at the time of annihilation (ref. 11, 16 and 17). The binding energy of the electron can lower the gamma-ray energy as much as 10 eV below the rest mass equivalent energy of an electron (511.003 keV), and the amount of this shift will depend on the material in which the positron finds the electron.

More importantly, the energy of the annihilation gamma ray can vary by as much as 1 keV because of the possible range of residual momentum at the time of annihilation. Because this energy variability is of the order of the energy resolution one expects at 511 keV with a HPGe detector, there will be a noticeable broadening of the 511 keV peak width. The effect is commonly referred to as Doppler Broadening of the peak shape. The amount of Doppler Broadening depends on the material in which the positron is annihilating, and on conditions that affect the population of available electrons in the material. Consequently, Doppler Broadening is one of the techniques used with positron sources to study chemical states, stress and microscopic voids in materials (ref. 16 and 17).

The energy shift and Doppler Broadening make positron annihilation a useful tool for studying materials. But, when performing an energy calibration and resolution check on a HPGe detector, the 511 keV annihilation radiation from a radioactive  $^{22}\text{Na}$  source can be misleading.  $^{22}\text{Na}$  has a half life of 2.60 years. It decays by positron emission (90%) or electron capture (10%) to the 1.2746 MeV excited state of  $^{22}\text{Ne}$ . The lifetime of the excited state is 3 picoseconds. Consequently, emission of the 1.2746 MeV gamma ray is a prompt signal that either electron capture or  $\beta^+$  decay has occurred. The end-point energy for the  $\beta^+$  decay to the excited state is 0.545 MeV. The positron has to lose most of the 0.545 MeV in the surrounding material before it has a high probability of being captured by an electron to cause the annihilation. That implies a maximum penetration depth of the order of a millimeter or less in metals. Near the end of the energy-loss process the positron annihilates with an

# High-Resolution Gamma-Ray Spectroscopy

electron. Obviously, the rate of energy loss and the range of the positron are going to depend on the absorbing material. The residual momentum at the time of annihilation also depends on local variations in the population of available electrons. Consequently, the Doppler Broadening will depend on the nature of the absorbing material.

In this experiment a thin  $^{22}\text{Na}$  source with minimal window thickness will be used. This enables the experimenter to sandwich the positron source between different absorbing materials to measure the Doppler Broadening on the 511 keV annihilation gamma rays. The thickness of aluminum required to stop the 0.545 MeV positrons is approximately 1 mm or 0.039 inches. For Nickel, the range of 0.545 MeV positrons is approximately 0.32 mm, or 0.013 inches. For both metals, the foil thicknesses actually employed will transmit 90% to 99% of the 511 keV gamma-rays that are generated.

## Procedure

1. This experiment will use the same spectrometer set-up as employed in Experiment IV-7.3, except the gain will be changed to place the 662 keV gamma-ray near the upper end of the energy spectrum on the MCA.
2. Remove all other sources from the vicinity of the HPGe detector, and place the  $^{137}\text{Cs}$  source at a distance that yields a percent dead time <63%.
3. Acquire a spectrum on the MCA and determine the channel number for the position of the 662 keV peak. If it is not within  $\pm 200$  channels of channel number 7400, adjust the amplifier gain to bring the peak position within those limits.
4. Ensure that the 662-keV peak has sufficient counts to enable an accurate measurement of its centroid position and the FWHM in channels. When determining the channel numbers that correspond to half the height of the peak, it will be helpful to interpolate to a tenth of a channel. Alternatively, a region of interest can be set over the peak, and MAESTRO can be used to measure the centroid and the FWHM. Record the peak position and the FWHM. Save the spectrum for possible later reference.
5. Remove the  $^{137}\text{Cs}$  source and replace it with the  $^{57}\text{Co}$  source. If necessary, adjust the source-to-detector distance so that the dead time is <63%.
6. Acquire a spectrum with sufficient counts to accurately measure the centroids of the 122 and 136.5 keV peaks. Save the spectrum for possible later reference.
7. Use the Energy Calibration feature of MAESTRO to calibrate the cursor to read in MeV or keV based on the peak positions from  $^{57}\text{Co}$  and  $^{137}\text{Cs}$ .

---

### EXERCISE

- a. Determine from the graph of experiment IV-7.1 the expected FWHM at an energy of 511 keV (note that your graph Y axis is the FWHM squared).
- 
8. Assemble the source and foil sandwich. From the FOIL-AL-30 kit place two aluminum foils on one side of the thin  $^{22}\text{Na}$  source for a total foil thickness of 1.5 mm on that side of the sandwich. Also apply two foils to the other side of the  $^{22}\text{Na}$  source to complete the symmetrical sandwich.
  9. Place the assembly in front of the detector on the axial centerline of the detector, with the foils parallel to the circular surface of the detector end cap. If necessary, adjust the sandwich-to-detector distance to ensure the dead time is <63%.
  10. Acquire a spectrum for a sufficient length of time to form a statistically well-defined peak at 511 keV. Save this spectrum for possible future reference.
  11. Set a region of interest (ROI) across the 511 keV peak. This peak sits on a background generated by the Compton continuum from the 1.2746 MeV gamma ray. Therefore, it is important to ensure that the limits of the ROI extend into that background on either side of the peak. Use the ROI features of MAESTRO to measure the peak position and FWHM in keV. Record those numbers.

---

### EXERCISES

- b. Compare the measured FWHM of the 511 keV peak with that determined in exercise a.

# High-Resolution Gamma-Ray Spectroscopy

- c. If the Doppler Broadening has a Gaussian distribution, the FWHM of that broadening can be computed from

$$\Delta E_{\text{DB}} = \sqrt{[\Delta E(511)_{\text{actual}}]^2 - [\Delta E(511)_{\text{predicted}}]^2}$$

Where  $\Delta E(511)_{\text{actual}}$  is the FWHM measured in step 13. Calculate  $\Delta E_{\text{DB}}$  for aluminum.

- d. Plot the profiles of the 662 keV peak and the 511 keV peak in the vicinity of each peak to compare the widths and symmetry. What differences do you see in peak shapes?
- e. How does the measured centroid for the 511 keV peak compare to the energy that would be expected if there were no shift from the binding energy of the electrons in aluminum, and no Doppler Broadening?
- .....

12. Repeat steps 10 through 13 and Exercises b. through e., with the sandwich assembled using two nickel foils from the Foil-Ni-10 kit on each side of the source, instead of the aluminum foils. The total nickel foil thickness on each side of the sandwich should be 0.51 mm.
- .....

## EXERCISE

- f. In addition to repeating Exercises b. through e. for nickel, compare the Doppler Broadening for the nickel to the Doppler Broadening for the aluminum. Nickel is reputed to have the largest Doppler Broadening compared to all the other pure metals in the annealed state. Are your measurements consistent with that expectation?
- g. Although not attempted in this experiment, it is well known that stressing a metal by repeated flexing, or by hammering the surface, causes additional Doppler Broadening. Subsequent annealing of the metal returns the Doppler Broadening to its lower value. What is a possible explanation for this phenomenon?
- .....

## References

1. A. Coche and P. Siffert, Lithium Drifted Silicon and Germanium Detectors in Semiconductor Detectors, G. Bertolini and A. Coche, Eds., Elsevier-North Holland, Amsterdam (1968).
2. J. C. Phillpott, IEEE Trans. Nucl. Sci. NS-17(3), 446(1970).
3. F. Adams and R. Dams, Applied Gamma Ray Spectrometry, 2nd Edition, Pergammon Press, Ltd.(1970).
4. U. E. P. Berg, H. Wolf, et al., Nucl. Instrum. Methods 129, 155 (1975).
5. C. Meixner, Nucl Instrum. Methods 119, 521 (1974).
6. D. M. Walker and J. M. Palms, IEEE Trans. Nucl. Sci. NS-17(3), 296 (1970).
7. M. L. Stelts and J. C. Browne, Nucl. Instrum. Methods 133, 35 (1976).
8. 20th Nuclear Science Symposium, IEEE Trans. Nucl. Sci. NS-21(1) (1974).
9. 19th Nuclear Science Symposium, IEEE Trans Nucl. Sci. NS-20(1) (1973).
10. C. M. Lederer and V. S. Shirley, Eds., Table of Isotopes, 7th Edition, John Wiley and Sons, Inc., New York (1978).
11. G. F. Knoll, Radiation Detection and Measurement, John Wiley and Sons, Inc., New York (1979).
12. Nuclear Data Sheets, Edited by the Nuclear Data Project, Elsevier Publishing, Inc. See also: [www.nndc.bnl.gov](http://www.nndc.bnl.gov)
13. See: Introduction to Semiconductor Photon Detectors at [www.ortec-online.com/Products-Solutions/RadiationDetectors/Overview.aspx](http://www.ortec-online.com/Products-Solutions/RadiationDetectors/Overview.aspx)
14. See: Introduction to Amplifiers and Introduction to CAMAC ADCs and Memories at [www.ortec-online.com/Products-Solutions/Modular-Electronic-Instruments-Overview.aspx](http://www.ortec-online.com/Products-Solutions/Modular-Electronic-Instruments-Overview.aspx)
15. Ron Jenkins, R. W. Gould, and Dale Gedcke, Quantitative X-ray Spectrometry, Marcel Dekker, Inc., New York, 1981.
16. Principles and Applications of Positron and Positronium Chemistry, Editors: Y. C. Jean, P.E. Mallon, and D. M. Shrader, World Scientific Publishing Co., Pte., Ltd., Singapore, 2003.
17. I. K. MacKenzie, Experimental Methods of Annihilation Time and Energy Spectrometry, Positron Solid-State Physics, LXXXIII Corso Soc. Italiana di Fisica, Bologna, Italy, 1983, pp 196 - 264.

Specifications subject to change  
071415

**ORTEC**<sup>®</sup>

[www.ortec-online.com](http://www.ortec-online.com)

Tel. (865) 482-4411 • Fax (865) 483-0396 • [ortec.info@ametek.com](mailto:ortec.info@ametek.com)

801 South Illinois Ave., Oak Ridge, TN 37830 U.S.A.

For International Office Locations, Visit Our Website

**AMETEK**<sup>®</sup>  
ADVANCED MEASUREMENT TECHNOLOGY